Physics Letters B 780 (2018) 211–215

Contents lists available at ScienceDirect

Physics Letters B

www.elsevier.com/locate/physletb

The nuclear contacts and short range correlations in nuclei

R. Weiss [a], R. Cruz-Torres [b], N. Barnea [a], E. Piasetzky [c], O. Hen [b,*]

[a] Racah Institute of Physics, Hebrew University, Jerusalem 91904, Israel
[b] Massachusetts Institute of Technology, Cambridge, MA 02139, USA
[c] School of Physics and Astronomy, Tel Aviv University, Tel Aviv 69978, Israel

ARTICLE INFO

Article history:
Received 5 August 2017
Received in revised form 24 November 2017
Accepted 22 January 2018
Available online 28 February 2018
Editor: W. Haxton

ABSTRACT

Atomic nuclei are complex strongly interacting systems and their exact theoretical description is a long-standing challenge. An approximate description of nuclei can be achieved by separating its short and long range structure. This separation of scales stands at the heart of the nuclear shell model and effective field theories that describe the long-range structure of the nucleus using a mean-field approximation. We present here an effective description of the complementary short-range structure using contact terms and stylized two-body asymptotic wave functions. The possibility to extract the nuclear contacts from experimental data is presented. Regions in the two-body momentum distribution dominated by high-momentum, close-proximity, nucleon pairs are identified and compared to experimental data. The amount of short-range correlated (SRC) nucleon pairs is determined and compared to measurements. Non-combinatorial isospin symmetry for SRC pairs is identified. The obtained one-body momentum distributions indicate dominance of SRC pairs above the nuclear Fermi-momentum.

The atomic nucleus is one of the most complex systems in nature. One of the main challenges in describing nuclei is understanding the short interparticle part of the nuclear wave function. The challenge stems from the complicated nucleon–nucleon interaction and the large density of the nucleus. The latter causes all the relevant scales of the system (nucleon size, average distance, and interaction range) to be comparable, making effective theoretical descriptions very demanding. On the other hand, detailed understanding of these short-range correlations (SRCs) is important for neutron-star structure and the nuclear symmetry energy [1–4], the bound nucleon and free neutron structure functions [5–10], neutrino-nucleus interactions and neutrino oscillation experiments [11–15], and more.

Current mean-field nuclear theories describe well various static properties of nuclei, but fail to describe the dynamic effects of SRCs. Ab-initio many-body calculations [16–21] are still limited to light nuclei and/or to soft interactions that regulate the short-range/high-momentum parts of the nuclear wave function. Therefore, effective theories are still needed to describe medium and heavy nuclei and to identify the main physical process at short distances [22–25].

In the last decade there was a significant progress in describing SRCs in dilute Fermi systems. It was shown that if the interaction range r_0 is much shorter than the average interparticle distance d, and the scattering length a_s, a *contact* theory can be used to describe the system [26–29]. A series of relations between different observables and the probability of finding a particle pair in a close proximity emerge. The contact theory was studied in great detail theoretically, and validated experimentally, for ultra-cold Fermi gases [26–36].

For nuclei, several experimental observations resemble those of cold atomic systems [37,38]. However, in nuclei, the short-range interaction is about 0.5–1.5 fm, the average distance between nucleons is about 2.5 fm, and the scattering length is about −20 fm and 5 fm for the spin-singlet and spin-triplet channels, respectively. Therefore, the possibility to generalize the contact theory to nuclear systems is not obvious. Nevertheless, a generalized nuclear theory was recently presented which addresses the factorization of the nuclear many-body wave function at short distances [39]. Few of its predictions were verified, yet more convincing theoretical and experimental results must be provided to prove that indeed it is adequate for describing nuclear SRCs.

Many features of nuclear SRCs are well known and should be properly explained by any candidate theory. Recent scattering experiments indicate that SRC pairs account for 20%–25% of the nu-

* Corresponding author.
E-mail address: hen@mit.edu (O. Hen).

https://doi.org/10.1016/j.physletb.2018.01.061

cleons in the nucleus and practically all nucleons with momentum above the Fermi momentum (k_F) [40–48]. They are predominantly in the form of neutron–proton (np) SRC pairs with large relative momentum ($k > k_F$), and small center-of-mass (c.m.) momentum ($K < k_F$). Here, $k_F \sim 255$ MeV/$c = 1.3$ fm^{-1} is the typical Fermi momentum of medium and heavy nuclei. These, and results of theoretical studies, indicate that the high-momentum ($k > k_F$) tail of the nuclear momentum distribution is dominated by SRC and described using a factorized wave function for the c.m. and relative momentum distributions of the pairs which results in similar two-body densities for different nuclei [22–25,49–54]. For recent reviews see [8,55]. Between these well-established properties and the generalized contact formalism there is a seemingly unsolved tension, as the latter's predictions involving two-body momentum distributions, are only satisfied for very high momentum, $k > 3k_F \approx 4$ fm^{-1}, and not for lower momentum $k_F < k < 3k_F$.

In this work, we will show that the generalized nuclear contact formalism can indeed describe SRCs in nuclei also in this lower momentum range. A direct agreement with both recent experimental data and with variational Monte Carlo (VMC) calculations will be presented. We will also discuss the nontrivial manner in which information on SRC is encapsulated in the nuclear two-body momentum distributions. The values of the nuclear contacts for various nuclei will be extracted using the VMC two-body distributions in coordinate and momentum space, separately, and also using experimental data. We find all three approaches to yield consistent values. Last, the VMC one-body momentum distributions are compared to the contact-formalism predictions, confirming the experimental observation that they are dominated by SRCs for momentum larger than k_F.

Generalized contact theory for nuclei – The original contact theory was formulated for systems with significant scale separation. Consequently, the Bethe–Peierls boundary condition can be used, leading at short interparticle distance to a factorized asymptotic wave-function of the form [29]:

$$\Psi \xrightarrow{r_{ij}\to 0} \varphi(\boldsymbol{r}_{ij}) A_{ij}(\boldsymbol{R}_{ij}, \{\boldsymbol{r}\}_{k\neq ij}). \tag{1}$$

Here $\varphi(\boldsymbol{r}_{ij})$ is an asymptotic two-body wave function, and A_{ij} is a function of the residual $A-2$ particle system. The scale separation allows replacing the short-range interaction with a boundary condition, and to ignore all partial waves but s-wave, leading to $\varphi(\boldsymbol{r}_{ij}) = (1/r_{ij} - 1/a_s)$. In momentum space, this factorized wave function leads to a high momentum tail, valid for $|a_s|^{-1}, d^{-1} \ll k \ll r_0^{-1}$, that is given by: $n(k) \to C/k^4$, where $C = 16\pi^2 \sum_{ij} \langle A_{ij}|A_{ij}\rangle$ is known as the *contact*.

To generalize this formalism to nuclear systems we need to consider two main points: (1) different partial waves might be significant, and therefore a sum over all possible nucleon–nucleon channels α must be introduced, and (2) as full scale separation does not exist, the asymptotic two-body channel wave-functions φ_α are taken from the solution of the nuclear zero-energy two-body problem. Therefore, the factorized asymptotic wave-function takes the form

$$\Psi \xrightarrow{r_{ij}\to 0} \sum_\alpha \varphi_\alpha(\boldsymbol{r}_{ij}) A_{ij}^\alpha(\boldsymbol{R}_{ij}, \{\boldsymbol{r}\}_{k\neq ij}) \,, \tag{2}$$

similar to the independent-pair approximation [56], where the index ij corresponds to pn, pp, and nn pairs [57].

In this work we will consider only the main channels contributing to SRCs, namely, the pn deuteron channel ($\ell = 0, 2$ and $s = 1$ coupled to $j = 1$) and the singlet pp, pn, and nn s-wave channel ($\ell = s = j = 0$). Using Eq. (2), asymptotic expressions for the one- and two-body momentum densities can be derived [39]:

$$\begin{aligned} n_p(\boldsymbol{k}) =& 2C_{pp}^{s=0}|\tilde{\varphi}_{pp}^{s=0}(\boldsymbol{k})|^2 + C_{pn}^{s=0}|\tilde{\varphi}_{pn}^{s=0}(\boldsymbol{k})|^2 \\ &+ C_{pn}^{s=1}|\tilde{\varphi}_{pn}^{s=1}(\boldsymbol{k})|^2 \end{aligned} \tag{3}$$

$$F_{pp}(\boldsymbol{k}) = C_{pp}^{s=0}|\tilde{\varphi}_{pp}^{s=0}(\boldsymbol{k})|^2$$

$$F_{pn}(\boldsymbol{k}) = C_{pn}^{s=0}|\tilde{\varphi}_{pn}^{s=0}(\boldsymbol{k})|^2 + C_{pn}^{s=1}|\tilde{\varphi}_{pn}^{s=1}(\boldsymbol{k})|^2 \tag{4}$$

and the same when replacing n with p. Here, C_{ij}^α are the nuclear contacts that determine the number of pairs in a given two-body channel, $n_N(\boldsymbol{k})$ is the one-body momentum distribution, and $F_{NN}(\boldsymbol{k})$ is the relative two-body momentum distribution. $F_{NN}(\boldsymbol{k}) = \int d\boldsymbol{K} F_{NN}(\boldsymbol{k}, \boldsymbol{K})$, where $F_{NN}(\boldsymbol{k}, \boldsymbol{K})$ is the probability of finding a pair of nucleons with relative momentum $\boldsymbol{k}$, and center-of-mass (c.m.) momentum $\boldsymbol{K}$. Similarly, $\rho_{NN}(\boldsymbol{r})$ describes the probability to find a pair of nucleons with relative distance $\boldsymbol{r}$. The subscripts N, and NN, stand for the type of nucleon/nucleon-pairs considered. Clearly, $n_{p(n)}(\boldsymbol{k}) = 2F_{pp(nn)}(\boldsymbol{k}) + F_{pn}(\boldsymbol{k})$ [39]. Equivalent two-body coordinate space densities for $\rho_{NN}(\boldsymbol{r})$ are given by replacing $\tilde{\varphi}(\boldsymbol{k})$ with $\varphi(\boldsymbol{r})$ in Eq. (4), while keeping the same nuclear contacts. We note that in deriving Eq. (3) the center-of-mass momentum of the pairs was assumed to be much smaller than k.

We choose to normalize $\tilde{\varphi}(\boldsymbol{k})$ such that $\int_{k_F}^\infty |\tilde{\varphi}(\boldsymbol{k})|^2 d\boldsymbol{k} = 1$. Using this normalization, and Eq. (3), the fraction of the one-body momentum density above k_F is given by:

$$\frac{\int_{k_F}^\infty n(\boldsymbol{k}) d\boldsymbol{k}}{\int_0^\infty n(\boldsymbol{k}) d\boldsymbol{k}} = \frac{C_{nn}^{s=0} + C_{pp}^{s=0} + C_{pn}^{s=0} + C_{pn}^{s=1}}{A/2}, \tag{5}$$

where $n(\boldsymbol{k}) = n_n(\boldsymbol{k}) + n_p(\boldsymbol{k})$, A is the number of nucleons in the nucleus and $C_{NN}^s/(A/2)$ gives the fraction of the one-body momentum density above the Fermi momentum due to each type of SRC pair.

Ab-initio nuclear two-body densities – Recent progress in quantum Monte-Carlo techniques allows performing ab-initio many-body calculations of nuclear structure for nuclei as heavy as ^{12}C [16,17]. Furthermore, cluster variational Monte-Carlo (CVMC) provides a way to obtain nuclear structure calculations for ^{16}O and ^{40}Ca [21]. These calculations are done using the AV18 and UX potentials, and result in one- and two-body nucleon densities in coordinate and momentum space.

The detailed study of the relation between two-body densities and two-nucleon knockout measurements is only now starting [39,49,50].

When examining the two-body densities at high relative momentum, certain care should be taken to separate SRC pairs from non-correlated pairs with high relative momentum. Two nucleons that form an SRC pair are close to each other, each have high momentum, their relative momentum is high, and their c.m. momentum is low. However, not all nucleon pairs with high relative momentum are necessarily SRC pairs. For example, a particle with momentum $k_1 \approx 4k_F$, and any uncorrelated "mean-field" particle at rest $k_2 \approx 0$, will yield a pair with high relative momentum $k \approx 2k_F$, and c.m. momentum $K \approx 2k_F$. In such cases, the high c.m. momentum is a signature for uncorrelated pairs. As we examine pairs with larger and larger relative momentum, this scenario becomes less and less probable as the probability of finding a nucleon with high momentum falls fast with the momentum, i.e. its easier to find two nucleon with momentum $\approx 2k_F$ then one nucleon with momentum $\approx 4k_F$.

There are two ways to access regions in the two-body momentum distribution dominated by SRC pairs, with minimal mean-field nucleon contamination. One is to integrate over the pairs c.m. momentum but request a very large relative momentum, which ensures that the pair is truly an SRC pair. This explains why Ref. [39] observed scaling between the one and two-body densities only for momentum much larger than k_F. The alternative approach is to

Table 1
The nuclear contacts for a variety of nuclei. The contacts are extracted by fitting the asymptotic expressions of Eq. (4) to the VMC two-body densities in momentum (k) and coordinate (r) space separately. For ^{4}He and ^{12}C the contacts extracted from electron scattering data are also shown. The nuclear contacts are divided by A/2 and multiplied by 100 to give the percent of nucleons above k_F in the different SRC channels.

A	k-space				r-space			
	$C_{pn}^{s=1}$	$C_{pn}^{s=0}$	$C_{nn}^{s=0}$	$C_{pp}^{s=0}$	$C_{pn}^{s=1}$	$C_{pn}^{s=0}$	$C_{nn}^{s=0}$	$C_{pp}^{s=0}$
^{4}He	12.3±0.1	0.69±0.03	0.65±0.03		11.61±0.03	0.567±0.004		
	14.9±0.7 (exp)	0.8±0.2 (exp)						
^{6}Li	10.5±0.1	0.53±0.05	0.49±0.03		10.14±0.04	0.415±0.004		
^{7}Li	10.6 ± 0.1	0.71 ± 0.06	0.78 ± 0.04	0.44 ± 0.03	9.0 ± 2.0	0.6 ± 0.4	0.647 ± 0.004	0.350 ± 0.004
^{8}Be	13.2±0.2	0.86±0.09	0.79±0.07		12.0±0.1	0.603±0.003		
^{9}Be	12.3±0.2	0.90±0.10	0.84±0.07	0.69±0.06	10.0±3.0	0.7±0.7	0.65±0.02	0.524±0.005
^{10}B	11.7±0.2	0.89±0.09	0.79±0.06		10.7±0.2	0.57±0.02		
^{12}C	16.8±0.8	1.4±0.2	1.3±0.2		14.9±0.1	0.83±0.01		
	18±2 (exp)	1.5±0.5 (exp)						
^{16}O					11.4±0.3	0.68±0.03		
^{40}Ca					11.6±0.3	0.73±0.04		

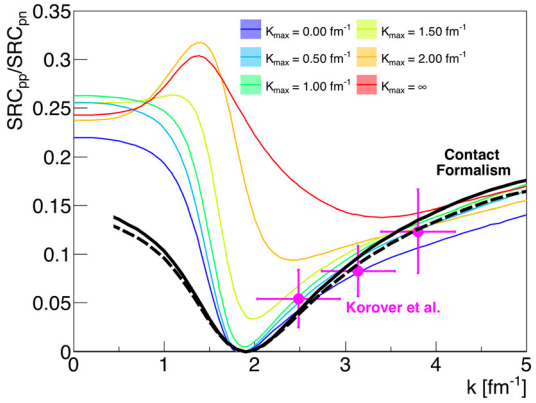

Fig. 1. The ratio of proton–proton to proton–neutron SRC pairs in ^{4}He as a function of the pair momentum extracted from ^{4}He(e,e'pN) measurements [47]. The colored lines show the equivalent ab-initio two-body momentum densities ratio integrated over the c.m. momentum from 0 to K_{max} that varies from zero to infinity [16]. The solid (dashed) black line is the contact theory prediction calculated using the contacts extracted in momentum (coordinate) space (Eq. (7)). (For interpretation of the colors in the figure(s), the reader is referred to the web version of this article.)

consider pairs with high relative momentum $\boldsymbol{k}$, and low c.m. momentum $\boldsymbol{K}$. The cut on $\boldsymbol{K}$ reduces the contributions from mean field nucleons significantly, and identifies SRC pairs with lower relative momentum. It should be noted that in the limit of heavy nuclei the contribution of uncorrelated nucleon pairs with low c.m. momentum could increase.

These two approaches can be demonstrated by comparing the two-body density calculations to data. Fig. 1 shows the calculated and measured proton–proton (pp) to proton–neutron (pn) pairs density ratio in ^{4}He as a function of their relative momentum. The experimental data are obtained from recent electron induced two-nucleon knockout measurements performed in kinematics dominated by breakup of SRC pairs [47]. The calculated pair density ratio is shown as a function of the relative pair momentum and is given by: $\int_0^{K_{\max}} d\boldsymbol{K}\, F_{pp}(\boldsymbol{k},\boldsymbol{K}) / \int_0^{K_{\max}} d\boldsymbol{K}\, F_{np}(\boldsymbol{k},\boldsymbol{K})$, where K_{max} varies from zero to infinity. As can be seen, as long as the maximal c.m. momentum is small, i.e. $K_{max} < 1$–1.5 fm$^{-1} \sim k_F$, the calculated ratio describes well the experimental data for $k > k_F$. This demonstrates the above second approach. These results are inline with those of Ref. [49]. On the other hand, demonstrating the first approach, if we concentrate on very high relative momentum, i.e. $k > 4$ fm^{-1}, we can see that the ratios are largely insensitive to the value of K_{max}.

Equipped with these observations, we are now in position to utilize the two-body densities to extract the values of the nuclear contacts.

Extracting the nuclear contacts – As explained above, we consider four main nuclear contacts: singlet $\ell = 0$ pn, pp, and nn, and triplet pn deuteron channel. For symmetric nuclei, spin-zero pp and nn pairs are identical, leaving three nuclear contacts: $C_{nn}^{s=0}$, $C_{pn}^{s=0}$, and $C_{pn}^{s=1}$. Isospin symmetry can be used to relate the various $s = 0$ contacts, leaving two independent contacts: spin-singlet and spin-triplet. For what follows, we do not impose isospin symmetry in order to study its manifestation in the case of SRC pairs.

We will extract the values of the contacts for nuclei up to ^{40}Ca in three different methods. In the first two methods we use the available two-body densities [16], in momentum space and coordinate space, separately. In the third method, we use experimental data. The results are summarized in Table 1, where one can see a good agreement between all three methods.

In the first (second) method, the values are extracted by fitting the factorized two-body momentum (coordinate) space expressions of Eq. (4) to the equivalent two-body density obtained from many-body VMC calculations [16]. The $s = 0$ pp and nn contacts are obtained by fitting the VMC pp and nn two-body density respectively. The $s = 1$ and $s = 0$ pn contacts are obtained from simultaneously fitting the spin–isospin $ST = 10$ pn two-body density and the total pn two-body density. In view of the discussion above, the fitting range was 4 fm^{-1} to 4.8 fm^{-1}, as $F_{NN}(\boldsymbol{k})$ is dominated by SRC pairs only for $k > 4$ fm^{-1}. In coordinate space the fitting was done in the range from 0.25 fm to 1 fm. The determination of the uncertainties is described in [57]. As VMC coordinate space distributions are not available for the different spin–isospin states, we assumed isospin symmetry (i.e. equal $s = 0$ contacts) for the symmetric nuclei. The universal functions φ_{ij}^{α} were calculated using the AV18 potential [57].

Experimentally, the nuclear contacts can be evaluated using the measured pp-to-pn SRC pairs ratio discussed above, $\frac{SRC_{pp}}{SRC_{pn}}(k)$, and the high-momentum scaling factor, $a_2(A/d)$. The latter is extracted from large momentum transfer inclusive electron scattering cross-section ratios and determines the relative number of high-momentum ($k > k_F$) nucleons in a nucleus, A, relative to deuterium [9,40–43], assuming the effects of Final-State Interactions and other reaction channels are suppressed in the kinematics of these measurements due to the large momentum transfer and the use of cross-section ratios, see Ref. [8,55] and references therein for

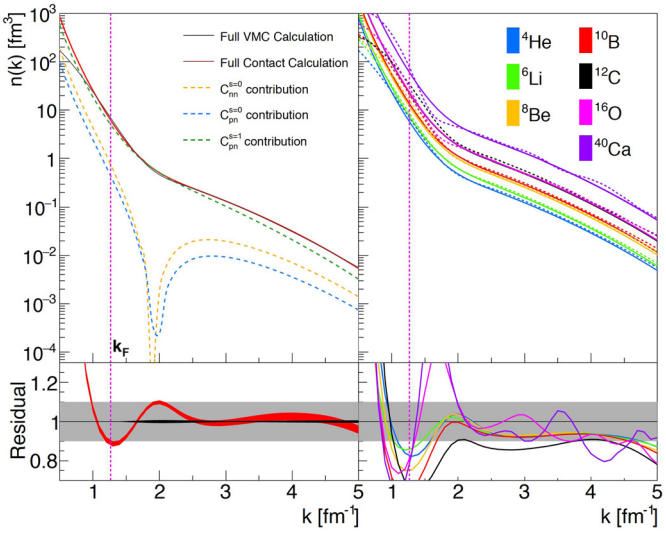

Fig. 2. (left) ^{4}He one-body momentum densities extracted from ab-initio VMC calculations (solid black band) and using the nuclear contact formalism (solid red band). The dashed lines show the contribution of different channels to the total contact calculation, using the contacts extracted in momentum space. The residual plot shows the ratio of the contact calculations to the VMC. The shaded region marks the 10% agreement region. The width of the black and red lines represents the individual uncertainties in the calculations. (right) The same, without error bands, comparing VMC calculations (dashed lines) and the nuclear contact formalism (solids lines) for different nuclei. The contacts used to calculate the distributions on the right plot were extracted in coordinate space.

details. Within the contact formalism, these experimental quantities can be expressed as:

$$a_2(A/d)\int_{k_F}^{\infty}|\tilde{\psi}_d(\boldsymbol{k})|^2 d\boldsymbol{k} = \frac{C_{nn}^{s=0}+C_{pp}^{s=0}+C_{pn}^{s=0}+C_{pn}^{s=1}}{A/2} \tag{6}$$

$$\frac{SRC_{pp}}{SRC_{pn}}(k) = \frac{C_{pp}^{s=0}|\tilde{\varphi}_{pp}^{s=0}(k)|^2}{C_{pn}^{s=0}|\tilde{\varphi}_{pn}^{s=0}(k)|^2 + C_{pn}^{s=1}|\tilde{\varphi}_{pn}^{s=1}(k)|^2} \tag{7}$$

where $\tilde{\psi}_d(\boldsymbol{k})$ is the deuteron wave function, normalized to one. In Eq. (7) it is assumed that the c.m. motion of SRC pairs is small, and similar for the different types of pairs in a given nucleus, as observed experimentally [46–48,58]. The experimental values of the contacts, shown in Table 1, were extracted for symmetric nuclei using these relations, assuming isospin symmetry.

The agreement between the values of the contacts that were extracted in momentum and coordinate space, points to a quantitative equivalence between high-momentum and short-range physics in nuclear systems. The agreement with the experimental extraction is an important indication for the validity of the contact formalism to nuclear systems. Another interesting feature of the extracted values is that, for symmetric nuclei, the momentum space $s=0$ pp and pn contacts are the same within uncertainties, in contrast to combinatorial expectations.

We can now utilize the values of the contacts to further investigate the predictions of the theory. First, we note that as the relation between the contacts and the one body momentum distribution, given in Eq. (3), was not used to fit the values of the contacts it can be considered as a verifiable prediction. Fig. 2 compares, for several nuclei, the one-body momentum distribution obtained from many-body VMC calculations to the prediction of Eq. (3). As can be seen, the asymptotic 1-body density, as predicted by the contact theory, reproduces with 10%–20% accuracy the many-body calculation starting from k_F to 5 fm^{-1}, where the momentum density varies over 3 orders of magnitude. It is worth emphasizing that even though the contacts fitting range was only $k > 4$ fm^{-1} using the two-body momentum distribution, the one-body momentum distribution is reproduced starting from k_F, as expected.

The contacts can also be used to calculate the pp to pn SRC pairs ratio using Eq. (7). This ratio can be compared with experimental electron induced two-nucleon knockout data [44–48] as shown for ^{4}He in Fig. 1. A similar comparison for ^{12}C [46] also shows a good agreement [57]. We can see that the contact predictions are in a good agreement with the experimental results and ab-initio calculations.

The contact formalism also allows us to evaluate the contributions of the different two-body channels to SRC pairs. Such decomposition is shown in Fig. 2 (left panel) for ^{4}He. The values of the contacts clearly show the expected dominance of the deuteron channel in SRC pairs. The fact that the contact formalism reproduces the VMC one-body momentum density to 10%–20% accuracy, without utilizing the spin–isospin $ST = 11$ channels, indicates their small importance to SRCs in the nuclei considered here. This stands in contrast to other works that do find a non-negligible contribution of $ST = 11$ pairs [59,60]. A possible explanation for this difference goes back to our discussion of the regions where the two-body momentum distribution describes SRCs. In these two papers, the c.m. momentum was not limited to small values and, thus, contributions from non-correlated pairs are expected to be significant. The contact theory provides a simple framework to perform such decompositions for SRC channels.

Conclusions – Even though nuclear systems do not strictly fulfill the scale-separation conditions required by the contact theory, both ab-initio one body momentum distribution above k_F and the experimental data are well reproduced using factorized asymptotic wave-functions and nuclear contact theory.

Consistent contacts extracted by separately fitting coordinate and momentum space two-body densities show equivalence between high-momentum and short-range dynamics in nuclear systems. Experimental extraction of the contacts gives also similar results. The values of the contacts allow a proper analysis of the spin–isospin quantum numbers of SRC pairs, and also reveal the non-combinatorial isospin-spin symmetry of SRCs.

This work provides clear evidence for the applicability of the generalized contact formalism to nuclear systems, and open the path towards further SRC studies.

Acknowledgements

We would like to thank B. Bazak, W. Cosyn, C. Ciofi degli Atti, S. Gandolfi, G. Miller, E. Pazi, J. Ryckebush, M. Sargsian, M. Strikman, and L.B. Weinstein for many fruitful discussions. This work was supported by the Pazy foundation, the Israel Science Foundation (grant no. 136/12, and 1334/16), and the U.S. Department of Energy Office of Science, Office of Nuclear Physics program under award number DE-FG02-94ER40818.

Appendix A. Supplementary material

Supplementary material related to this article can be found online at https://doi.org/10.1016/j.physletb.2018.01.061.

References

[1] L. Frankfurt, M. Sargsian, M. Strikman, Int. J. Mod. Phys. A 23 (2008) 2991.
[2] O. Hen, B.-A. Li, W.-J. Guo, L.B. Weinstein, E. Piasetzky, Phys. Rev. C 91 (2015) 025803.
[3] B.-J. Cai, B.-A. Li, Phys. Rev. C 93 (2016) 014619, arXiv:1509.09290 [nucl-th].
[4] O. Hen, A.W. Steiner, E. Piasetzky, L.B. Weinstein, arXiv:1608.00487 [nucl-ex], 2016.

[5] L.B. Weinstein, E. Piasetzky, D.W. Higinbotham, J. Gomez, O. Hen, R. Shneor, Phys. Rev. Lett. 106 (2011) 052301.
[6] O. Hen, A. Accardi, W. Melnitchouk, E. Piasetzky, Phys. Rev. D 84 (2011) 117501.
[7] O. Hen, D.W. Higinbotham, G.A. Miller, E. Piasetzky, L.B. Weinstein, Int. J. Mod. Phys. E 22 (2013) 1330017, arXiv:1304.2813 [nucl-th].
[8] O. Hen, G.A. Miller, E. Piasetzky, L.B. Weinstein, Rev. Mod. Phys. 89 (2017) 045002, arXiv:1611.09748 [nucl-ex].
[9] O. Hen, E. Piasetzky, L.B. Weinstein, Phys. Rev. C 85 (2012) 047301.
[10] J.-W. Chen, W. Detmold, J.E. Lynn, A. Schwenk, arXiv:1607.03065 [hep-ph], 2016.
[11] H. Gallagher, G. Garvey, G.P. Zeller, Annu. Rev. Nucl. Part. Sci. 61 (2011) 355.
[12] L. Fields, et al., MINERvA Collaboration, Phys. Rev. Lett. 111 (2013) 022501.
[13] G.A. Fiorentini, et al., MINERvA Collaboration, Phys. Rev. Lett. 111 (2013) 022502.
[14] R. Acciarri, et al., Phys. Rev. D 90 (2014) 012008.
[15] L.B. Weinstein, O. Hen, E. Piasetzky, Phys. Rev. C 94 (2016) 045501, arXiv:1604.02482 [hep-ex].
[16] R.B. Wiringa, R. Schiavilla, S.C. Pieper, J. Carlson, Phys. Rev. C 89 (2014) 024305.
[17] J. Carlson, S. Gandolfi, F. Pederiva, S.C. Pieper, R. Schiavilla, K.E. Schmidt, R.B. Wiringa, Rev. Mod. Phys. 87 (2015) 1067, arXiv:1412.3081 [nucl-th].
[18] G. Hagen, et al., Nat. Phys. 12 (2015) 186, arXiv:1509.07169 [nucl-th].
[19] A. Rios, A. Polls, W.H. Dickhoff, Phys. Rev. C 79 (2009) 064308, arXiv:0904.2183 [nucl-th].
[20] A. Rios, A. Polls, W.H. Dickhoff, Phys. Rev. C 89 (2014) 044303, arXiv:1312.7307 [nucl-th].
[21] D. Lonardoni, A. Lovato, S.C. Pieper, R.B. Wiringa, Phys. Rev. C 96 (2017) 024326, arXiv:1705.04337 [nucl-th].
[22] J. Ryckebusch, M. Vanhalst, W. Cosyn, J. Phys. G, Nucl. Part. Phys. 42 (2015) 055104.
[23] M. Vanhalst, J. Ryckebusch, W. Cosyn, Phys. Rev. C 86 (2012) 044619.
[24] C. Colle, et al., Phys. Rev. C 92 (2015) 024604.
[25] C. Ciofi degli Atti, S. Simula, Phys. Rev. C 53 (1996) 1689, arXiv:nucl-th/9507024.
[26] S. Tan, Ann. Phys. 323 (2008) 2952.
[27] S. Tan, Ann. Phys. 323 (2008) 2971.
[28] S. Tan, Ann. Phys. 323 (2008) 2987.
[29] E. Braaten, in: W. Zwerger (Ed.), The BCS-BEC Crossover and the Unitary Fermi Gas, Springer, Berlin, 2012.
[30] S. Gandolfi, K.E. Schmidt, J. Carlson, Phys. Rev. A 83 (2011) 041601.
[31] J.T. Stewart, J.P. Gaebler, T.E. Drake, D.S. Jin, Phys. Rev. Lett. 104 (2010) 235301.
[32] E.D. Kuhnle, H. Hu, X.-J. Liu, P. Dyke, M. Mark, P.D. Drummond, P. Hannaford, C.J. Vale, Phys. Rev. Lett. 105 (2010) 070402.
[33] G. Partridge, K. Strecker, R. Kamar, M. Jack, R. Hulet, Phys. Rev. Lett. 95 (2005) 020404.
[34] F. Werner, L. Tarruell, Y. Castin, Eur. Phys. J. B 68 (2009) 401.
[35] A. Schirotzek, Radio-Frequency Spectroscopy of Ultracold Atomic Fermi Gases, Ph.D. thesis, Massachusetts Institute of Technology, 2010.
[36] Y. Sagi, T. Drake, R. Paudel, D. Jin, Phys. Rev. Lett. 109 (2012) 220402.
[37] O. Hen, L.B. Weinstein, E. Piasetzky, G.A. Miller, M.M. Sargsian, Y. Sagi, Phys. Rev. C 92 (2015) 045205.
[38] R. Weiss, B. Bazak, N. Barnea, Phys. Rev. Lett. 114 (2015) 012501.
[39] R. Weiss, B. Bazak, N. Barnea, Phys. Rev. C 92 (2015) 054311, arXiv:1503.07047 [nucl-th].
[40] L. Frankfurt, M. Strikman, D. Day, M. Sargsyan, Phys. Rev. C 48 (1993) 2451.
[41] K. Egiyan, et al., CLAS Collaboration, Phys. Rev. C 68 (2003) 014313.
[42] K. Egiyan, et al., CLAS Collaboration, Phys. Rev. Lett. 96 (2006) 082501.
[43] N. Fomin, et al., Phys. Rev. Lett. 108 (2012) 092502.
[44] A. Tang, et al., Phys. Rev. Lett. 90 (2003) 042301.
[45] E. Piasetzky, M. Sargsian, L. Frankfurt, M. Strikman, J.W. Watson, Phys. Rev. Lett. 97 (2006) 162504.
[46] R. Subedi, et al., Science 320 (2008) 1476.
[47] I. Korover, N. Muangma, O. Hen, et al., Phys. Rev. Lett. 113 (2014) 022501, arXiv:1401.6138 [nucl-ex].
[48] O. Hen, et al., CLAS Collaboration, Science 346 (2014) 614.
[49] M. Alvioli, C. Ciofi degli Atti, H. Morita, Phys. Rev. C 94 (2016) 044309, arXiv:1607.04103 [nucl-th].
[50] M. Alvioli, C. Ciofi Degli Atti, L.P. Kaptari, C.B. Mezzetti, H. Morita, Int. J. Mod. Phys. E 22 (2013) 1330021, arXiv:1306.6235 [nucl-th].
[51] T. Neff, H. Feldmeier, W. Horiuchi, Phys. Rev. C 92 (2015) 024003.
[52] L.L. Frankfurt, M.I. Strikman, Phys. Rep. 76 (1981) 215.
[53] L. Frankfurt, M. Strikman, Phys. Rep. 160 (1988) 235.
[54] J.L. Forest, V.R. Pandharipande, S.C. Pieper, R.B. Wiringa, R. Schiavilla, A. Arriaga, Phys. Rev. C 54 (1996) 646, arXiv:nucl-th/9603035.
[55] C. Ciofi degli Atti, Phys. Rep. 590 (2015) 1.
[56] L.C. Gomes, J.D. Walecka, V.F. Weisskopf, Ann. Phys. 3 (1958) 241.
[57] Online supplementary matterials, 2016.
[58] R. Shneor, et al., Phys. Rev. Lett. 99 (2007) 072501.
[59] H. Feldmeier, W. Horiuchi, T. Neff, Y. Suzuki, Phys. Rev. C 84 (2011) 054003, arXiv:1107.4956 [nucl-th].
[60] M. Alvioli, C. Ciofi degli Atti, L.P. Kaptari, C.B. Mezzetti, H. Morita, Phys. Rev. C 87 (2013) 034603, arXiv:1211.0134 [nucl-th].